

2024

## Co-firing of LPG and Diesel Fuels through an Innovative Double Swirl Burner: Combustion characteristics and Exhaust Emissions

Eslam O. Mater

*Department of Mechanical Power Engineering, Faculty of Engineering Mattaria, Helwan University, Egypt,*  
eslam.osama285@gmail.com

Karim M. Soliman

*Department of Mechanical Power Engineering, Faculty of Engineering, Cairo University, Cairo, Egypt*

A. Abdulnaim

*Department of Mechanical Power Engineering, Faculty of Engineering Mattaria, Helwan University, Egypt*


Ahmed Abdelrazik Emara

*Department of Mechanical Power Engineering, Faculty of Engineering Mattaria, Helwan University, Egypt*

Ahmed Salah Elsahy

*Department of Mechanical Power Engineering, Faculty of Engineering, Zagazig University, Ash Sharqiyah, Egypt*

Follow this and additional works at: <https://tast.researchcommons.org/journal>

 *next page for additional authors*  
Part of the [Heat Transfer, Combustion Commons](#)

---

### How to Cite This Article

Mater, Eslam O.; Soliman, Karim M.; Abdulnaim, A.; Emara, Ahmed Abdelrazik; Elsahy, Ahmed Salah; and Moneib, Hany A. (2024) "Co-firing of LPG and Diesel Fuels through an Innovative Double Swirl Burner: Combustion characteristics and Exhaust Emissions," *Trends in advanced sciences and technology*. Vol. 1, Article 3.

DOI: 10.62537/2974-444X.1001

Available at: <https://tast.researchcommons.org/journal/vol1/iss1/3>

This Original Study is brought to you for free and open access by Trends in Advanced Sciences and Technology. It has been accepted for inclusion in Trends in advanced sciences and technology by an authorized editor of Trends in Advanced Sciences and Technology.

---

# Co-firing of LPG and Diesel Fuels through an Innovative Double Swirl Burner: Combustion characteristics and Exhaust Emissions

## Authors

Eslam O. Mater, Karim M. Soliman, A. Abdulnaim, Ahmed Abdelrazik Emara, Ahmed Salah Elsahy, and Hany A. Moneib

## ORIGINAL STUDY

# Co-firing of Liquefied Petroleum Gas and Diesel Fuels Through an Innovative Double Swirl Burner: Combustion Characteristics and Exhaust Emissions

Eslam Osama Mater<sup>a,b,\*</sup>, Karim Mohamed Soliman<sup>c</sup>, Ahmed Mohamed Abdulnaim<sup>a</sup>, Ahmed Abdelrazik Emara<sup>a</sup>, Ahmed Salah Elsayh<sup>d</sup>, Hany Ahmed Moneib<sup>a</sup>

<sup>a</sup> Department of Mechanical Power Engineering, Faculty of Engineering Mattaria, Helwan University, Egypt

<sup>b</sup> Department of Mechanical Engineering, Faculty of Engineering, Badr University, Egypt

<sup>c</sup> Department of Mechanical Power Engineering, Faculty of Engineering, Cairo University, Cairo, Egypt

<sup>d</sup> Department of Mechanical Power Engineering, Faculty of Engineering, Zagazig University, Ash Sharqiyah, Egypt

## Abstract

The current stringent environmental regulations, the depletion of fossil fuels and the emergence of oil biofuels and synthetic gases had motivated combustion scientists to search for alternative technologies that meet efficient burning, flexible use of multiple fuels, and conform to a clean environment. In that respect, several developments had emerged including, low swirl combustion for partially premixed mixtures and 'mild' combustion for diffusion flames. The present experimental study introduces a new concept that combines separate admissions of fuel and air with a central recirculation zone following the diffusion combustion mode, partial premixing within a premix chamber resulting in the creation of a uniform and dispersed reaction zone having a uniform distributed temperature with diminished temperature peaks, leading to low NO<sub>x</sub> and CO emissions. In that respect, this work investigates experimentally the flame flow field of co-firing diesel and liquefied petroleum gas (LPG) in terms of the combustion characteristics and exhaust emissions at a fixed loading condition of 20 kW while varying equivalence ratio ( $\phi$ ) between 0.6 and 0.9. Three co-firing cases of liquid fuel/gaseous fuel ratios of 90/10, 80/20, and 70/30 based on energy share are compared with the standalone diesel combustion. A coaxial burner is designed and manufactured with a central pressure jet atomizer housed inside a vane swirler. This set is coaxially surrounded by an annulus gaseous hub feeding 12 angularly spaced gaseous jets. A coaxial vane swirler is fitted at the outer annulus area. A conical premix chamber is mounted at the burner gun exit to direct the outer swirling airstream to the flame core. The burner is coaxially fitted to a water-cooled horizontal cylindrical combustion chamber. At a higher equivalence ratio ( $\phi = 0.9$ ), increasing the LPG ratio shows a clear reduction in CO emissions compared with standalone diesel combustion. However, at a lower equivalence ratio ( $\phi = 0.6$ ), the LPG ratio has a minor influence on the CO level. On the contrary, NO<sub>x</sub> concentration reaches its peak value with the increase of the gaseous fuel share in energy. The cumulative heat transfer to the combustor walls is always higher in the co-firing test cases due to the relatively higher radiation and convection heat transfer modes. Optimal conditions are achieved at liquid fuel/gaseous fuel ratios = 70/30, exhibiting the lowest CO emissions (~30 ppm), adequate NO<sub>x</sub> levels (~15 ppm), and the highest cumulative heat flux (~55% of input load at  $\phi = 0.9$ ) among all the test cases.

**Keywords:** Coaxial burners, Co-firing, Diffusion flames, Exhaust emissions, Swirling flames

## 1. Introduction

The co-firing concept had previously received greater research attention and implementation regarding combustion in diesel engines utilizing

natural gas as the main fuel, which is pilot ignited by diesel injection near the end of the compression stroke (Abedin et al., 2016; Cheenkachorn et al., 2013; Wannatong et al., 2007). This concept is currently receiving progressive interest for

Received 12 December 2023; revised 25 January 2024; accepted 26 January 2024.  
Available online 20 May 2024

\* Corresponding author. Mechanical Power Engineering Department, Faculty of Engineering Mattaria, Helwan University, Cairo, 11718, Egypt.  
E-mail addresses: [islam.usama@buc.edu.eg](mailto:islam.usama@buc.edu.eg), [eslam.osama285@gmail.com](mailto:eslam.osama285@gmail.com) (E.O. Mater).

<https://doi.org/10.62537/2974-444X.1001>

2974-444X/© 2024, Helwan University. This is an open access article under the Creative Commons Attribution-NonCommercial-NoDerivatives licence (CC BY-NC-ND 4.0).

applications in furnaces and boilers to replace traditional single or dual fuel burners. The latter is commonly designed to operate at one fuel at a time due to complications in control strategies associated with complicated burner mapping that raise difficulties in the proper setting of the twin fuel feed lines to satisfy the requirements of flame stabilization, combustor efficiency, and environmental regulations at any one load (Baukal, 2003). Recently, more concern has been given to co-firing due to worldwide interest in increasing the renewable energy share in the energy mix policies. In that respect, biofuel and syngas (generated from waste) seemed to have more significant potential to generate efficient renewable thermal energy (energy at a higher temperature) (Taibi et al., 2012) that not only complies with the environmental regulations suggested by the Paris Agreement (Agreement, 2015, p. 2017) but also reduces the reliance on the depleted conventional fossil fuels.

Co-firing of liquid and gaseous fuels can be accomplished through diffusion (Adam et al., 2022) or premixed (Valera-Medina et al., 2017) or partially premixed modes of combustion. In either mode, a modified coaxial burner is used. In the diffusion mode, the oil fuel is centrally admitted through either (i) a pressure jet atomizer, (ii) an air-assisted atomizer, or (iii) a steam-assisted atomizer. The combustion air is admitted coaxially through a central stabilizer disk or a coaxial vane swirler for flame stabilization. The gaseous fuel is fed through a surrounding coaxial annulus hub to interact with the central oil spray. The gaseous stream may fully pass through the annulus exit area or be injected through multiple radially distributed gas nozzles. An outer air stream (swirling or nonswirling) may be incorporated to envelop the developed flame.

As to the premixed mode of combustion, the same design configuration of the oil fuel line with the central coaxial air admittance is kept unchanged while a swirling premixed gaseous/air stream passes through the outer annulus area. In either mode of combustion, a conical premix chamber may be fitted at the exit of the burner gun to inwardly direct the outer swirling air (in the case of the diffusion mode) or the swirling gaseous premixed stream (in the case of the diffusion mode) for better mixing.

Regarding partially premixed combustion, a controlled quantity of premixed fuel and air is introduced into the combustion chamber, giving rise to a partially homogeneous mixture. The ensuing combustion process is distinguished by flame propagation, presenting prospects for

#### Nomenclature

$\dot{m}_{oil}$	diesel fuel mass flow rate cc(kg/h)
$\dot{m}_{air}$	combustion air mass flow rate (kg/h)
$\dot{m}_{gas}$	LPG fuel mass flow rate (kg/h)
$x$	axial distance along the combustor starting from the burner exit (m)
$D$	combustor inner diameter (m)
$Q_c$	cumulative heat transferred to combustor walls (kW)

enhanced thermal efficiency and reduced emissions of pollutants.

An advantage point of co-firing liquid fuel with gaseous fuel is that the heat produced from the gaseous flame will result in faster vaporization of liquid fuel droplets leading to better mixing with the combustion air, and hence higher reaction rate, rapid oxidation of CO and soot and intense shorter flame and efficient combustion (Al-Omari et al., 2010). The heat consumed in the early vaporization of oil droplets (by the gaseous fuel) would result in rapid devolatilization of the fuel droplets and rapid mixing with the combustion air resulting in a higher reaction rate and hence higher flame temperature leading to rapid oxidation of the soot particulate. The rapid diminishing of the soot particles (lower emissivity) is superseded by the higher attainable temperature, resulting in higher radiation transfer and hence a shorter flame.

Another benefit of co-firing is that the main heat transfer mode of liquid fuel flames is radiation mode due to high soot formation (Coelho, 2017), while the thermal heat of gaseous flames is transferred mainly by convection. Therefore, co-firing has the advantage of heat transfer by both convection and radiation. Moreover, co-firing flames of biofuels and syngas have low heat release rates due to lower heating values of both fuels and higher viscosity, which cause poor atomization with relatively large droplet size and a low percentage of combustible elements in syngas. That's why it is feasible to apply the concept of co-firing with conventional oil and gas for efficient, stable burning together with relatively lower emissions, for example,  $\text{NO}_x$  and CO.

Exhaust emission and mapping the rich and lean flame stability limits of co-firing diesel and syngas were investigated by Agwu and Valera-Medina (2020). Runs were carried out at  $\phi = 0.7$  and a combined heat output of 15 kW. It is found that the increase in the percentage of syngas at the expense of diesel percentage reduction causes CO to increase while  $\text{NO}_x$  decreases exhaust emissions.

Also, flame stability increases with increasing syngas percentage.

Another study by [Chong et al. \(2020\)](#) examines co-firing of palm methyl esters/diesel fuel and natural gas at a constant input thermal power of 9.3 kW, while the equivalence ratio varied between 0.65 and 0.9. Liquid fuel is sprayed into the combustor by an air-assisted atomizer while natural gas is premixed with air and admitted through axial swirl (45° vane angle). Their results showed high CO and NO emissions when operating on palm methyl esters/natural gas. Also, at  $\phi = 0.65$  lower CO level is noticed with higher NO compared with the levels produced at  $\phi = 0.9$ .

Another biodiesel co-firing study conducted by [Kurji et al. \(2017\)](#) used diesel or biodiesel co-fired with a blend of natural gas and carbon dioxide in a swirl burner with a central liquid fuel atomizer of 0.4 GPH (gallon per hour) capacity. Combustion air is premixed with natural gas and is introduced to the combustion chamber using an axial swirl. The heating power was kept constant at 20 kW, while the equivalence ratio varied from 1.4 to 2.1. The results showed a clear reduction in CO and NO<sub>x</sub> emissions in all test cases for biodiesel blends across all measurements. Also, flame temperature and reaction rate are reduced by injecting carbon dioxide, leading to decreasing NO<sub>x</sub> emission.

Also, there is a study of local extinction specifications of methane/ethanol co-firing by [Sidey and Mastorakos \(2017\)](#). Their study uses a co-firing burner with a central pressure atomizer surrounded by a stream of methane premixed with air through an axial vane swirl. In all test cases, air and liquid fuel flow rates are held constant, while the gaseous fuel flow rate is altered. Two reference test cases (pure ethanol and pure methane) are compared with four dual fuel co-firing cases at a lean equivalence ratio. The study showed that increasing the gaseous fuel flow rate reduces the air/fuel range of stable flame and increases the probability of flame lift.

Co-firing of waste cooking oil or kerosene with natural gas was investigated by [Altaher et al. \(2012\)](#). The used burner comprises a radial injector for producing central biodiesel spray and two corotating radial swirlers. Natural gas fuel injection orifices were mounted centrally on the wall of the swirler outlet throat. Runs were carried out at a constant amount of natural gas, while the equivalence ratio was altered between 0.18 and 0.34 using the central injection of biodiesel or kerosene. The results show that biodiesel performs excellently in a co-firing mode, but not good in standalone burning. Also, NO<sub>x</sub> emissions produced by co-firing biodiesel and natural gas were higher than pure natural gas.

The concept of double swirl is investigated by [Elbaz et al. \(2019\)](#) through the utilization of liquefied petroleum gas (LPG) in a double swirl staged burner, assessing flame stability, NO emissions, and flame structure. The burner equipped with concentric outer and annular swirlers around a central jet allows control of mixing by varying swirl angles and equivalence ratios. Results indicate that LPG admitted through the annular mixture enhances flame stability more than the outer mixture, with central fuel injection further improving stability. Reduced segregation between annular and outer streams leads to lower NO emissions. The flame features distinct zones, including a recirculation zone where high NO concentration is limited.

As mentioned previously, the application of dual fuel co-firing in industrial burners has not been extensively studied. To address this gap, this study focuses on utilizing LPG and light diesel oil (fossil fuels) in an innovative co-firing double swirl burner to assess the new burner design and combustion characteristics and establish a reference base with which future work on biofuels could be compared. The use of double swirl in a staged burner firing premixed gaseous fuels (inner rich core with outer lean streams) had been previously proved to yield low NO<sub>x</sub> and CO emissions. In parallel, the present study adopts a quite similar configuration, but with a central oil fuel and a coflowing outer gaseous stream. Focus is given to studying the combustion performance and emissions at a constant heat input of 20 kW and varying ranges of equivalence ratio (0.6–0.9) and liquid/gas ratio (LGR).

## 2. Experimental test facilities and program

### 2.1. Experimental test rig

[Fig. 1](#) shows a schematic diagram of the present experimental setup. It consists of a horizontal cylindrical water-cooled combustor having an inner diameter of 160 mm and a length of 1000 mm. It is constructed from a 6 mm thick sheet metal. The cooling jacket has an outer diameter of 200 mm and is segmented into three consecutive sections with progressive lengths to allow adequate mapping of the longitudinal variations of the total heat flux distribution. Forty axial measuring taps of 10 mm bore diameter are made to allow the insertion of various measuring probes. These taps are closely distributed (2 cm apart) at the upstream segment to facilitate adequate mapping of the flame structure. The end side of the combustor is connected to a stack chimney to transfer the exhaust to the atmosphere. A twin fuel, double swirl burner, [Fig. 2](#), is coaxially mounted

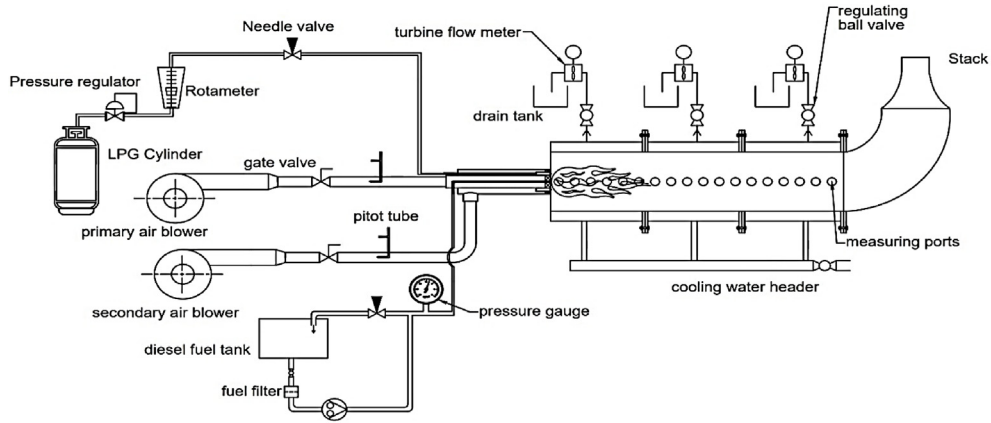
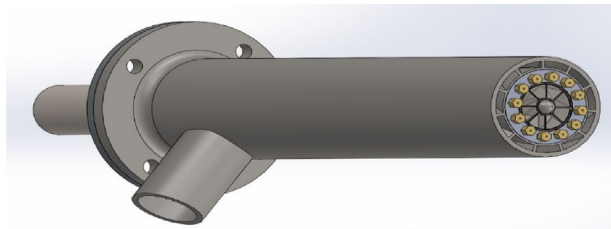


Fig. 1. Schematic diagram of the test setup.

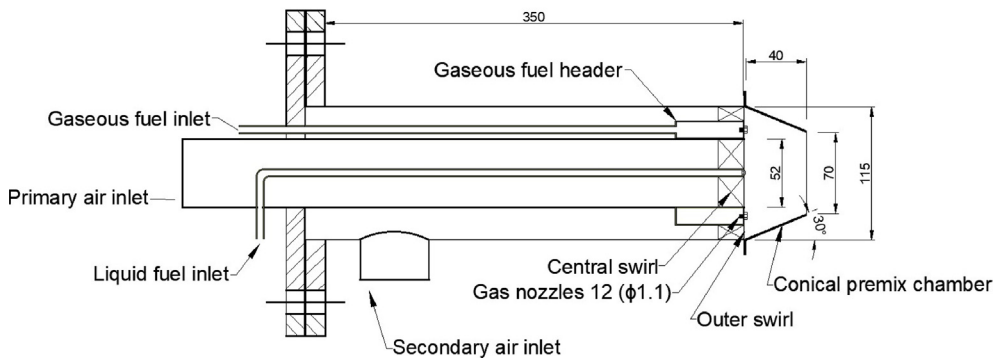
at the combustor entry. The burner gun has an outer diameter of 115 mm that houses (at its exit) a central pressure jet atomizer (solid cone, 0.45 GPH, 45°) being fitted to an inner vane swirler having an outer diameter of 52 mm and a swirl angle of 60° providing a recirculation zone necessary to flame stabilization (Chiong et al., 2020). It is coaxially surrounded by an annulus gas supply passage that feeds 12 hexagonal gaseous nozzles (1.1 mm orifice diameter each) that are circumferentially equally spaced at a diameter of 68 mm. An outer vane swirler with an inner diameter of 85 mm and a vane angle of 60° (same direction as the inner swirler) fits onto the remaining annulus

space of the burner gun. A conical premix chamber with a 30° tapered angle and 70 mm outlet diameter is fitted at the exit of the burner gun not only to enhance the premixing of the gaseous and oil streams but also to inwardly direct the outer swirling air stream to the flame core. This burner configuration (with double swirlers) facilitates early rapid interactions between air, gaseous, and oil streams as previously recommended by the following (Elbaz et al., 2019; Tung et al., 2015) compared with a single swirl.

The air stream is supplied from a centrifugal blower (3 HP) through a 2-inch pipe and controlled



Panel (a) Burner configuration (without exit conical premix chamber)



Panel (b) Burner schematic

Fig. 2. Burner design details.



by a gate valve measured by a standard pitot tube connected to a differential pressure sensor. The air mass flow rate is accurate to within  $\pm 1\%$ . The gaseous fuel line (LPG) comprises pressure bottles and a pressure regulator. A needle valve controls its flow rate and monitors it with a calibrated Siargo MF 5706 gas flow meter to an accuracy of  $\pm 0.5\%$ . Diesel fuel is supplied from a storage tank through an oil filter to a gear pump. Its mass flow rate is set using a bourdon tube pressure gauge being calibrated using primary standards (via recording the time needed to collect an oil mass of 0.5 kg at a given oil pressure).

## 2.2. Measuring techniques

Several measuring techniques are being used at the integral and the macroscopic level, namely:

- (1) An S-type thermocouple of 120  $\mu\text{m}$  wire diameter and 150  $\mu\text{m}$  hot junction diameter to measure the axial mean gas temperature of the flames. The thermocouple wires are housed inside a twin-bore ceramic (2 mm OD) tube surrounded by a stainless-steel tube (6 mm OD). Omega universal thermocouple connector (UTC-USB) with built-in thermocouple cold junction compensation and linearization and accuracy of  $\pm 0.5\%$  FS links the thermocouple with the PC to provide a digital temperature reading. For each measured point, an average of 30 readings is taken at 30 s to ensure the accuracy of the measurement. Radiation loss is ignored following the finding reported by MMA et al. (1980).
- (2) Heat transferred from the flame to combustor walls is measured by monitoring the cooling water total enthalpy increase at each section through measuring the cooling water flow rate and temperature rise. The former is measured using a calibrated turbine flow sensor SEN0217 (1–30 l/min, accuracy:  $\pm 5\%$ ) connected to an Arduino linked to an LCD for a flow rate digital display. The latter is measured using a K-type thermocouple located at discharge and wired to a UNI-T (UT320A) thermocouple reader with an accuracy of  $\pm 0.5\% + 1^\circ$ .
- (3) The inflame dry volumetric gas analysis of  $\text{NO}_x$ , CO, and  $\text{CO}_2$  is measured using an 'Ampro 2000' gas analyzer (electrochemical cells) with accuracies of: CO low less than 4000 ppm:  $\pm 10$  ppm, CO high (0–4%):  $\pm 0.02\%$ , and  $\text{NO}_x$ :  $\pm 2.0$  and  $\text{CO}_2$ :  $\pm 0.3\%$ . The gas samples are withdrawn using a stainless-steel water-cooled probe having an outer diameter of 6 mm and a sampling tube of 2 mm. The withdrawn sample is sucked using a sealed vacuum pump and is dried and freed from dirt using a cotton wool filter and a coarse silica gel.

## 2.3. Experimental program

The experimental program shown in Table 1 considers the operating conditions for all test runs under two modes of firing namely, (i) light diesel oil firing (reference cases, R1–R4) and (ii) co-firing of LDO and LPG fuels (three test cases) (physicochemical properties given in Table 2) whereby the value of LGR is gradually varied by increasing the gaseous fuel flowrate at the expense of decreasing

Table 1. Experimental program.

#	Fuel type	LGR	Heat input (kW)	$\dot{m}_{oil}$ (kg/h)	$\dot{m}_{gas}$ (kg/h)	$\phi$	$\dot{m}_{air}$ (kg/h)
R1	LDO (reference case)	100/0	20	1.69		0.9	27.2
R2						0.8	30.6
R3						0.7	35.0
R4						0.6	40.8
A1	Co-fire (LDO + LPG)	80/20		1.52	0.155	0.9	27.2
A2						0.8	30.6
A3						0.7	35.0
A4						0.6	40.8
B1	Co-fire (LDO + LPG)	80/20		1.35	0.313	0.9	27.2
B2						0.8	30.5
B3						0.7	34.9
B4						0.6	40.7
C1	Co-fire (LDO + LPG)	70/30		1.18	0.468	0.9	27.1
C2						0.8	30.5
C3						0.7	34.9
C4						0.6	40.7

LPG, liquefied petroleum gas.

Table 2. Physiochemical properties for used fuels.

Property	Diesel	LPG
Calorific value (mj/kg)	44	48.5
Density (kg/m <sup>3</sup> ) at 25 °C	834	1.898
Kinematic viscosity (mm <sup>2</sup> /s) at 40 °C	2.6	—
Stoichiometric air-fuel ratio	14.3	15.2

LPG, liquefied petroleum gas.

the liquid fuel throughput while maintaining a constant heat input of 20 kW. In all cases, the overall equivalence ratio is varied from 0.6 to 0.9.

The present experimental program aims to investigate the variations of the inflame thermal and chemical structure, the cumulative heat transfer to the combustor cooling jacket, and the exhaust emissions associated with the changes in LGR value in co-firing cases. This data is to be compared with the standalone burning of liquid fuel. The thermal structure is indicated through measuring the inflame mean gas temperature while the chemical structure is acquired through the measurements of the inflame dry volumetric analysis of CO and NO<sub>x</sub>. The inflame temperature is measured at eight axial positions, while inflame species concentrations are measured at 10 axial positions. The selection of measurement positions based on multiple measurements to identify locations where significant fluctuations in the measured property occurred. The program is complemented by studying (i) the variation of inflame temperature, (ii) exhaust emissions (CO<sub>2</sub>, CO, and NO<sub>x</sub>), and (iii) the cumulative heat transfer to the combustor cooling jacket. Therefore, 16 test cases are carried out to achieve sufficient data for the required investigation.

### 3. Results and discussion

#### 3.1. On-axis variations of the inflame thermal and chemical structure

##### 3.1.1. Axial variations of the mean gas temperature

Fig. 3 shows axial variations of the inflame mean gas temperature at the combustor centerline for the four LGRs at  $\phi = 0.8$ .

Examining the four profiles may indicate the following:

(1) The pure diesel flame exhibits a temperature of 920 °C at the immediate exit of the conical premix chamber, which is followed by a gradual rise reaching a maximum of only 1000 °C at  $x/D = 0.75$ . Considering that the present atomizer gives a solid cone spray with dense core droplets that interact with a central recirculation zone of hot combustion products created by the inner and outer swirlers

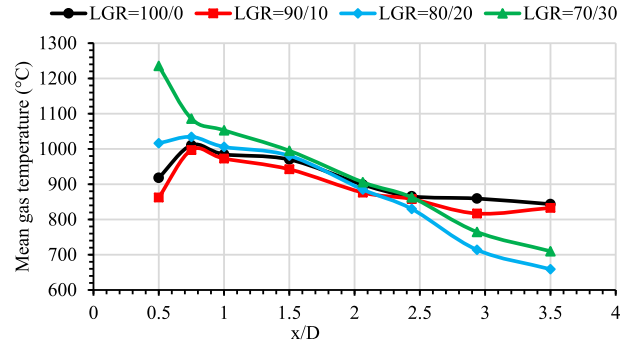


Fig. 3. Axial variations of the mean flame gas temperature inside the combustor at different values of LGR at  $\phi = 0.8$ .

suggests an oxygen-deficient environment (lower reaction rate) that led to partial vaporization and oxidation of the core droplets and hence to a lower maximum flame temperature. This is followed by a gradual decline in the flame temperature due to radiation loss. Moreover, it has been observed that the temperature gradient downstream of the combustor is comparatively higher in the absence of partial preheating, leading to a higher visible flame length. This, in turn, results in an increased residence time of diesel droplets and a consequent delay in their complete vaporization, which is consistent with previous findings (Jiang & Agrawal, 2014).

- (2) At a low gas share of LGR = 90/10, there is a modest reduction of the flame temperature along the combustor length when compared with the pure diesel flame. This can be attributed to the reduction in the oil atomizing pressure that leads to the formation of slightly coarser oil droplets and hence a decline in fuel pyrolysis on one hand. On the other hand, these droplets are partially preheated by the surrounding annulus gaseous jet flames. The net result is a slight drop of around less than or equal to 40 °C.
- (3) At the intermediate gas share of LGR = 80/20, the on-axis mean temperature experienced a further increase to reach 1040 °C at the exit of the premix chamber. This suggests a rise in the rate of fuel pyrolysis and partial oxidation due to the extra preheating by the gaseous jet flames and enhancement in combustion quality attributed to improved atomization. The middle part of the flame experienced gradual heat radiation loss. It is followed by a steeper drop in temperature as the visible flame length terminates at  $x/D \sim 2.5$ .
- (4) At a high gas ratio LGR = 70/30, the on-axis mean gas temperature at the exit of the premix chamber experienced a rapid rise reaching 1240 °C; signaling rapid vaporization, premixing, and



preheating at the dense core of the spray cone together with heat released by the burnout of the gaseous jets. The achieved maximum temperature just mentioned is certainly governed by the amount of heat needed to vaporize the fuel droplets.

### 3.1.2. Axial variations of species concentrations of CO and NO<sub>x</sub>

Fig. 4 presents the axial variations of the inflame dry volumetric gas analyses of CO and NO<sub>x</sub> species concentration at a fixed value of  $\phi = 0.8$  and varying LGR. The presented data are compared with the reference test case of pure oil flame (LGR = 100/0). The following conclusions and explanations may be withdrawn:

- (1) At the immediate of the burner conical premix chamber ( $x/D = 0.3$ ), the pure oil flame (LGR = 100/0) exhibits the highest level of CO of 3%. On the contrary, the progressive increase of the gaseous fuel throughout the co-firing test cases seems to promote oil fuel vaporization and partial oxidation within the premix chamber that ultimately (at LGR = 70/30) lowered the CO level to 0.3% and increased the level of NO<sub>x</sub> to reach its highest level of 94 ppm at  $x/D = 0.6$ .

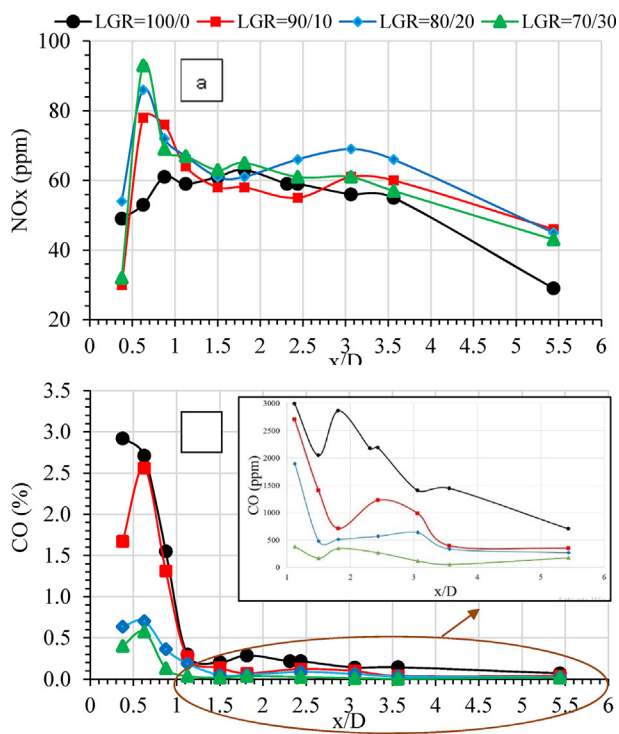


Fig. 4. Axial variations of the inflame dry volumetric analysis of species concentration of NO<sub>x</sub> (panel a) and CO (panel b) profiles at fixed equivalence ratio ( $\phi = 0.8$ ) and different LGR.

- (2) Further downstream ( $0.6 < x/D < 1.1$ ), all flames showed a rapid decline of CO and NO<sub>x</sub> (within the flame core). This indicates in a way faster conversion of CO to CO<sub>2</sub>, leading to a depletion of the availability of O<sub>2</sub> and higher dilution of the reaction zone by the combustion products that resulted in the decline of NO<sub>x</sub>.
- (3) At the remaining flame zone that follows ( $1.1 < x/D < 3.5$ ), axial variations of both NO<sub>x</sub> and CO levels exhibit a plateau profile. The former is at  $60 \pm 8$  ppm, while the level of the latter (300, 500, and 1000 ppm) rises with the increase of the value of LGR as shown in the attached graph in Fig. 4.
- (4) In the post-flame region both the levels of CO and NO<sub>x</sub> slowly decline due to the rise of O<sub>2</sub> level in the exhaust resulting from the excess air factor.

### 3.2. Exhaust gas emissions

Fig. 5 shows variations of the normalized dry volumetric emissions of CO, NO<sub>x</sub>, and CO<sub>2</sub> at a fixed thermal input of 20 kW and different values of the LGR and the overall equivalence ratio. The emissions are measured at the combustor stack, positioned at a height of 50 cm from the combustor level, and below the stack exit plane by 40 cm. Emission values for CO and NO<sub>x</sub> have been adjusted to a standard reference point, specifically normalizing at 15% oxygen levels in the flue gases. This normalization provides a standardized comparison, accounting for variations in oxygen content during measurements. The following findings and explanations may be withdrawn as follows:

- (1) The pure diesel flame: at the highest value of  $\phi = 0.9$ , CO exhibits the highest ever level of 1180 ppm which is coupled with 10% CO<sub>2</sub> and 7 ppm NO<sub>x</sub>. These indicate partial fuel oxidation. A progressive decrease of the value of  $\phi = 0.6$  (high excess air) results in a gradual decline of the CO and CO<sub>2</sub> to reach lower levels of 400 ppm and 7%, respectively, with a gradual rise of NO<sub>x</sub> to 12 ppm. These are indicative of progressive oxidation of the reactants being coupled with quenching by excess air dilution, which never led to combustion completion.
- (2) At the low gas share of LGR = 90/10: the oil spray cone experienced preheating by the surrounding annulus gas jets which led to faster oil fuel vaporization and oxidation as shown by the rapid decline of CO and increase of CO<sub>2</sub>. It is worth noting that the CO reaches a minimum of 200 ppm at  $\phi = 0.7$ , followed by a gradual rise to

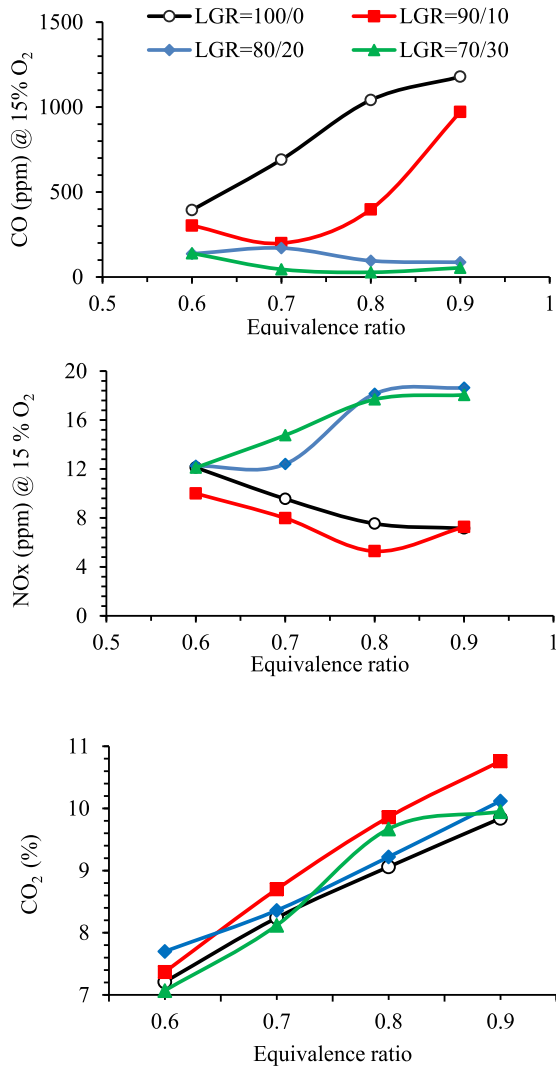


Fig. 5. Variations of the normalized dry volumetric emissions of CO, NO<sub>x</sub>, and CO<sub>2</sub> at different LGR for different values of the overall equivalence ratio (input thermal load = 20 kW).

300 ppm at  $\phi = 0.6$ . This finding indicates that  $\phi = 0.7$  denotes the optimum excess air above which the effect of air dilution prevails. It is also suggested that at equivalence ratios near stoichiometry ( $\phi = 0.8$ – $0.9$ ), inadequate mixing between air and fuel occurs. This is attributed to the air quantity being slightly above the required amount for complete combustion. Consequently, due to inadequate mixing and lower flame temperatures, incomplete combustion takes place as evident in high CO levels and low NO<sub>x</sub> levels. Moreover, as the combustion leans toward lower equivalence ratios ( $\phi = 0.7$ – $0.6$ ), the increased air quantity promotes combustion, resulting in lower CO levels as CO is oxidized to CO<sub>2</sub> and increasing NO<sub>x</sub>

emissions due to the abundance of oxygen in the combustion zone.

- (3) At the intermediate gas share of LGR = 80/20: at this percentage of the gaseous share, the flame temperature rises due to (i) the greater energy generated by burning the gaseous fuel in itself and (ii) the additional heat released by burning the oil droplets that experienced faster preheating, vaporization, and mixing. This is indicated by the rapid drop of CO to 90 ppm and rise of NO<sub>x</sub> to 18 ppm at  $\phi = 0.9$ . Progressive moving from the slightly leaner side ( $\phi = 0.9$ ) to the much leaner side ( $\phi = 0.6$ ) indicates a slight rise in normalized species concentrations of CO (90–170 ppm) and increased air dilution induces quenching effects, leading to lower flame temperatures and reduced combustion intensity. This suggestion is supported by CO levels rising and NO<sub>x</sub> levels declining.
- (4) At high gas ratio LGR = 70/30: additional injection of LPG results in similar trends of CO, NO<sub>x</sub>, and CO<sub>2</sub> to those just explained in (c) with slight differences in values. For example, CO drops by almost 100 ppm in comparison with case (c) above; reaching the lowest level  $\approx 40$ – $50$  ppm. As regards NO<sub>x</sub> little variations never exceeding 2 ppm may be detected between cases (c) and (d).

### 3.3. Cumulative heat transferred to the combustor cooling jacket

Figure 6 shows the percentage variations of the cumulative heat transfer ( $Q_c$ ) along the three segments of the combustor water jacket at a fixed thermal input varying values of LGR (including the reference oil burning case, LGR = 100/0) and different values of  $\phi$ .

The percentage heat transfer to a particular water jacket segment ( $Q_{c_{sn}}$ ) is given by

$$Q_{c_{sn}} = \frac{[m_w \times C_{p_w} \times (T_{w_{out}} - T_{w_{in}})]_{sn}}{Q_{input}} \times 100.$$

The percentage cumulative heat transfer ( $Q_c$ ) to the combustor cooling jackets is given by

$$Q_c = \sum_{sn=1}^n Q_{c_{sn}}$$

A thorough examination of Fig. 6 clearly shows that the maximum level of the value of  $Q_c$  in all test cases (of 54%) is achieved at  $\phi = 0.9$  and LGR = 70/30 as shown in panel a. This finding recommends (from the energy point of view regarding co-firing of oil and gas) the utilization of 30% of gas energy

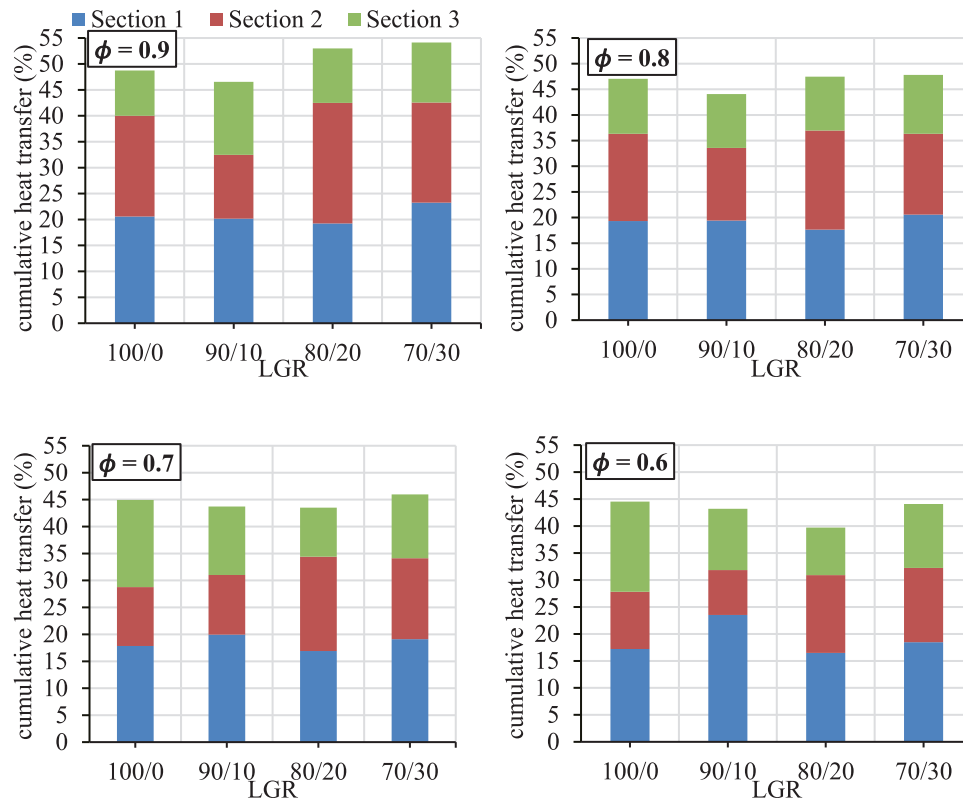


Fig. 6. Variations of the cumulative heat transfer ( $Q_c$ ) along the three segments of the combustor water jacket at varying values of LGR.

share in the co-firing of oil and gas (at an excess air factor of 10% ( $\phi = 0.9$ ) due to the noticeable increase in the in-flame temperature. This is also supplemented (from the environmental point of view) by the diminished level of CO emissions ( $\sim 50$  ppm) in exhaust, but at the expense of a slight rise in NO<sub>x</sub> (not exceeding 20 ppm) as shown earlier in Fig. 5. In addition, it is important to note that while the input heat is maintained at a constant 20 kW, the heat released varies in each test run due to different conditions in the combustion process.

#### 4. Conclusions

The present experimental study is focused on assessing (in terms of flame characteristics and exhaust emissions of CO and NO<sub>x</sub>), the relevance of employing co-firing of gaseous (LPG) and oil fuel (diesel) in comparison with burning a standalone oil fuel. In that respect, an experimental test stand comprising a cylindrical water-cooled combustor fitted with a novel coaxial burner is used. The burner gun housed a central pressure jet solid cone atomizer and two annular (central and outer) air vane swirlers with an intermediate annular section fitted with 12 circumferential gaseous jets. The exit

of the burner gun is fitted with a conical premix chamber. Experiments are conducted at a constant thermal input of 20 kW and varying (i) LGR = 100/0–70/30: energy basis and (ii) equivalence ratio ( $\phi = 0.9$ –0.6).

The following findings are withdrawn:

- (1) Co-firing at a low amount of LPG (LGR = 90/10) requires a reduction in oil atomizing pressure, which in turn lowers the overall temperature by  $\sim 40$  °C compared with pure diesel. Further injection of LPG causes extra preheating by the gaseous jet flames which promotes fuel pyrolysis and partial oxidation. This, in turn, leads to a significant increase in temperature, with a maximum temperature of 1240 °C achieved at LGR = 70/30.
- (2) The introduction of LPG promotes the preheating of the oil spray, leading to faster vaporization and oxidation of the oil fuel. This results in a rapid decline in CO levels and an increase in CO<sub>2</sub> and NO<sub>x</sub> emissions. For instance, at an LGR of 70/30 and  $\phi = 0.9$ , CO levels are reduced by up to 95% compared with pure diesel burning. Moving to a much leaner side ( $\phi = 0.6$ ), CO tends to reduce significantly for pure diesel and low gas share cases while NO<sub>x</sub> emissions exhibit

a slight increase. Therefore, from an emission perspective, operating with an intermediate to high share of gaseous fuel is more advantageous as these cases exhibit very low CO emissions, albeit with a slight increase in NO<sub>x</sub> emissions.

- (3) At an equivalence ratio near stoichiometry, more injection of LPG augments the heat transfer by convection which leads to increasing both the heat liberated and the cumulative heat transfer to the combustor walls. Specifically, at an LGR of 70/30, the cumulative heat transfer increased by 5% compared with pure diesel. In addition, increasing of injected LPG fuel to the combustion changes the way heat is transferred so that it depends more on convection, which is a simple approach to control heat transfer.

### Conflicts of interest

There are no conflicts of interest.

### References

- Abedin, M. J., Imran, A., Masjuki, H. H., Kalam, M. A., Shahir, S. A., Varman, M., & Ruhul, A. M. (2016). An overview on comparative engine performance and emission characteristics of different techniques involved in diesel engine as dual-fuel engine operation. *Renewable and Sustainable Energy Reviews*, *60*, 306–316.
- Adam, A., Shahein, M., & Moneib, H. (2022). Overall assessment of an innovative coaxial air-staged burner for cofiring of oil and gas. *Engineering Research Journal*, *173*, 316–331.
- Agreement P. (2015). *Paris agreement. Report of the conference of the parties to the United Nations framework convention on climate change (21st session, 2015: Paris)*. Retrieved December (Vol. 4).
- Agwu, O., & Valera-Medina, A. (2020). Diesel/syngas co-combustion in a swirl-stabilised gas turbine combustor. *International Journal of Thermofluids*, *3–4*, Article 100026.
- Al-Omari, S. A. B., Shaheen, A., Al Fakhr, A., Al-Hosani, A., & Al Yahyai, M. (2010). Co-firing used engine lubrication oil with LPG in furnaces. *Energy Conversion and Management*, *51*, 1259–1263.
- Altaher, M. A., Li, H., & Andrews, G. E. (2012). Co-firing of kerosene and biodiesel with natural gas in a low NO<sub>x</sub> radial swirl combustor. *Proceedings of the ASME Turbo Expo*, *1*, 557–567.
- Baukal, C. E., Jr. (Ed.). (2003). *Industrial burners handbook*. CRC Press.
- Cheenkachorn, K., Poornpipatpong, C., & Ho, C. G. (2013). Performance and emissions of a heavy-duty diesel engine fuelled with diesel and LNG (liquid natural gas). *Energy*, *53*, 52–57.
- Chiong, M. C., Valera-Medina, A., Chong, W. W. F., Chong, C. T., Mong, G. R., & Mohd Jaafar, M. N. (2020). Effects of swirler vane angle on palm biodiesel/natural gas combustion in swirl-stabilised gas turbine combustor. *Fuel*, *277*, Article 118213.
- Chong, C. T., Chiong, M. C., Ng, J. H., Tran, M. V., Valera-Medina, A., Józsa, V., & Tian, B. (2020). Dual-fuel operation of biodiesel and natural gas in a model gas turbine combustor. *Energy and Fuels*, *34*, 3788–3796.
- Coelho, P. J. (2017). Radiative transfer in combustion systems. *Handbook of Thermal Science and Engineering*, *16*, 1.
- Elbaz, A. M., Moneib, H. A., Shebil, K. M., & Roberts, W. L. (2019). Low NO<sub>x</sub>-LPG staged combustion double swirl flames. *Renewable Energy*, *138*, 303–315.
- Jiang, L., & Agrawal, A. K. (2014). Combustion of straight glycerol with/without methane using a fuel-flexible, low-emissions burner. *Fuel*, *136*, 177–184.
- Kurji, H., Valera-Medina, A., Okon, A., & Chong, C. T. (2017). Combustion and emission performance of CO<sub>2</sub>/CH<sub>4</sub>/biodiesel and CO<sub>2</sub>/CH<sub>4</sub>/diesel blends in a Swirl Burner Generator. *Energy Procedia*, *142*, 154–159.
- Hassan, M. M. A., Lockwood, F. C., & Moneib, H. A. (1980). Fluctuating temperature and mean concentration measurements in a vertical turbulent free jet diffusion flame. *La Rivista Dei Combustibili*, *38*, 357–372.
- Sidey, J., & Mastorakos, E. (2017). Visualisation of turbulent swirling dual-fuel flames. *Proceedings of the Combustion Institute*, *36*, 1721–1727.
- Taibi, E., Gielen, D., & Bazilian, M. (2012). The potential for renewable energy in industrial applications. *Renewable and Sustainable Energy Reviews*, *16*, 735–744.
- Tung, C., Shiung, S., & Hochgreb, S. (2015). Combustion performance of a counter-rotating double swirl flame burner under stratified burning condition. *Chemical Engineering Transactions*, *45*, 193–198.
- Valera-Medina, A., Marsh, R., Runyon, J., Pugh, D., Beasley, P., Hughes, T., & Bowen, P. (2017). Ammonia–methane combustion in tangential swirl burners for gas turbine power generation. *Applied Energy*, *185*, 1362–1371.
- Wannatong, K., Akarapanyavit, N., Siengsanorh, S., & Chanchaona, S. (2007). Combustion and knock characteristics of natural gas diesel dual fuel engine (No. 2007-01-2047). SAE Technical Paper.